Topological Waveguiding near an Exceptional Point: Defect-Immune, Slow-Light, and Loss-Immune Propagation

S. Ali Hassani Gangaraj* and Francesco Monticone†
School of Electrical and Computer Engineering, Cornell University, Ithaca, New York 14853, USA

(Received 11 March 2018; published 28 August 2018)

Electromagnetic waves propagating in conventional wave-guiding structures are reflected by discontinuities and decay in lossy regions. In this Letter, we drastically modify this typical guided-wave behavior by combining concepts from non-Hermitian physics and topological photonics. To this aim, we theoretically study, for the first time, the possibility of realizing an exceptional point between coupled topological modes in a non-Hermitian nonreciprocal waveguide. Our proposed system is composed of oppositely biased gyrotropic materials (e.g., biased plasmas or graphene layers) with a balanced distribution of loss and gain. To study this complex wave-guiding problem, we put forward an exact analysis based on classical Green's function theory, and we elucidate the behavior of coupled topological modes and the nature of their non-Hermitian degeneracies. We find that, by operating near an exceptional point, we can realize anomalous topological wave propagation with, at the same time, low group velocity, inherent immunity to backscattering at discontinuities, and immunity to losses. These theoretical findings may open exciting research directions and stimulate further investigations of non-Hermitian topological waveguides to realize robust wave propagation in practical scenarios.

DOI: 10.1103/PhysRevLett.121.093901

Introduction.—The ability of guiding light and electromagnetic waves in desired directions is of fundamental importance for science and technology, from long-haul optical fibers, to the possibility of on-chip optical interconnects [1], enhanced light-matter interactions at the micro- and nanoscale [2], as well as in the context of complex feeding networks for modern radars and 5G antenna systems [3]. Controlling wave propagation with more flexibility and robustness may lead to novel applications and advances in different domains of wave physics (electromagnetics, acoustics, seismic and elastic waves, etc.), including for invisibility and stealth technologies, robust defect- or damage-tolerant wave-guiding and radiating systems, and wave-based information processing [4].

Wave propagation in conventional wave-guiding structures is characterized by some typical properties that limit their behavior and applicability. (i) Conventional waveguides support modes that are allowed to propagate in either directions with equal and opposite wave vectors, $|k_+(\omega)| = |k_-(\omega)|$; i.e., they are symmetric upon time reversal, a consequence of the Lorentz reciprocity theorem for most media and structures [5]. As a result, any defect and discontinuity in the waveguide is allowed to excite a backward-propagating wave. (ii) Typical waveguide modes exhibit moderately large group velocity $\partial\omega/\partial k$, hence, limited interaction time with matter. Specific dispersion-engineering strategies are necessary to slow light down [6]. (iii) Waveguide modes decay in lossy regions, which obviously limits their propagation length. More generally, it is typically accepted that, in longitudinally homogeneous waveguides, the amplitude of a guided mode, $\propto |e^{-i\omega t}e^{i\mathbf{k}\cdot\mathbf{r}}|$, with respect to the direction of propagation is either a constant function if the waveguide is closed and lossless or an exponential function if the waveguide is lossy or gainy.

In this Letter, we theoretically propose a wave-guiding structure that violates all three points outlined in the previous paragraph at the same time, based on combining concepts from non-Hermitian physics and topological photonics. This may lead to the realization of anomalous guided-wave propagation exhibiting backscattering immunity, loss immunity, and low group velocity simultaneously. To realize this exciting possibility, we present for the first time an *exact* analysis of coupled unidirectional modes in non-Hermitian topological wave-guiding structures based on Green's function theory, which reveals the presence and nature of an exceptional point (EP) where two topologically protected modes coalesce. Such a topological non-Hermitian degeneracy is the key to the anomalous propagation properties described above.

Topological non-Hermitian wave-guiding.—Our general discussion is based on a continuum model of a photonic topological insulator with broken time-reversal symmetry (a Chern-type insulator) [7,8], but our considerations can be extended to any type of photonic topological materials [9–11]. In particular, we consider a homogeneous or effective gyrotropic material, which can be described by permittivity and permeability tensors: $\underline{\boldsymbol{\epsilon}} = \epsilon_0(\epsilon_t\mathbf{I}_t + \epsilon_a\hat{\mathbf{z}}\,\hat{\mathbf{z}} + i\epsilon_g\hat{\mathbf{z}}\times\mathbf{I})$, $\underline{\boldsymbol{\mu}} = \mu_0\mathbf{I}$, where $\mathbf{I}_t = \mathbf{I} - \hat{\mathbf{z}}\,\hat{\mathbf{z}}$ ($\mathbf{I}$ is the unit tensor), with ε_g

being the magnitude of the gyration pseudovector. A continuous gyrotropic material can be realized, e.g., by a plasma magnetically biased along a given direction (in our case, the z axis) with frequency-dispersive permittivity elements having a certain plasma frequency ω_p and cyclotron frequency ω_c [12,13]. It has been known since at least the 1960s that, when a gyrotropic material is interfaced with a different medium, under certain conditions a unidirectional backscattering-immune surface mode emerges [25]. In recent years, the nature and origin of this mode has been related to the nontrivial topological properties of the gyrotropic material [26–29]. In particular, for the case of a magnetized plasma, the gap Chern number is equal to unity [27]; therefore, at the interface with a topologically trivial material, exactly one topologically protected one-way edge state emerges.

In order to study a configuration with coupled topological modes, we then consider a layered wave-guiding structure as in Fig. 1(a), composed of a topologically trivial isotropic layer of thickness h and permittivity ϵ_r sandwiched between two gyrotropic media with permittivity tensors $\underline{\boldsymbol{\epsilon}}_i$, $i = 1, 2$, which we name TNT (topological nontopological topological) waveguide. The two gyrotropic media, e.g., magnetized plasmas, are oppositely biased in order to have unidirectional transverse-magnetic surface waves propagating in the same direction, as shown in Fig. 1(b). The two surface waves are topologically protected and can couple if the two interfaces are sufficiently close [30,31].

The exact Green's function of the structure can be expressed as a Fourier integral with respect to the transverse momentum k_x [13]. In the central region of the TNT waveguide, assuming the frequency of operation lies within

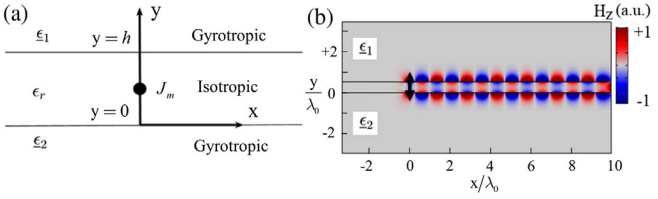

FIG. 1. (a) Topological wave-guiding structure composed of two oppositely biased gyrotropic media separated by an isotropic layer (J_m indicates a current source). (b) Example of magnetic field distribution (time snapshot) propagating in a lossless (Hermitian) topological waveguide as in (a), excited by a dipolar source (black arrow). The magnetic field is normalized to its maximum value. Two unidirectional surface waves propagate along the interfaces and couple through the isotropic layer. For this example, we assumed $\omega_{p,1} = \omega_{p,2} = 0.9\omega_0$, $\epsilon_r = -1$, and $\omega_{c,1} = -\omega_{c,2} = 0.28\omega_0$, where ω_0 is the source frequency. The width of the isotropic layer is $0.55\lambda_0$, where λ_0 is the free-space wavelength at ω_0. Throughout the Letter, we have purposely normalized all parameters in the figures by wavelength and plasma frequency; our designs can, therefore, be scaled to any size and frequency range of interest.

the band gap of the biased plasmas, this integral can be evaluated as a sum of residue terms corresponding to the unidirectional guided modes of the waveguide, as follows:

$$H_z(x,y) = 2\pi i \sum_m w^{spp}(k_{mx},\omega) e^{ik_{mx}x}, \tag{1}$$

where $w^{spp}(k_x,\omega) = N(k_x,\omega)/\partial_{k_x} D(k_x,\omega)$ is the complex amplitude of the mode, and the functions N and D are defined in Ref. [13]. k_{mx} is the mth root (mth guided-wave pole) of the dispersion equation of the system $D(k_x,\omega) = 0$ for a given set of parameters $(\omega, h, \omega_{pi}, \omega_{ci})$. If the system is closed (Hermitian) with no decaying channels (intrinsic loss or radiation), the modes of the waveguide are orthogonal [32], whereas, if the system is open, two (or more) modes may perfectly coalesce and become linearly dependent at an EP [33–37].

To study the non-Hermitian topological case, we introduce loss and gain into the gyrotropic layers of the TNT waveguide. Mathematically, this can be obtained by modifying the frequency-dependent elements of the permittivity tensors as $\epsilon_{1,j}(\omega + i\delta, \omega_p, \omega_c)$ and $\epsilon_{2,j}(\omega + i\delta', \omega_p, \omega_c)$, where $j = t, a, g$. By choosing $\delta = -\delta'$, we realize a balanced (parity-time-symmetric) configuration. The trajectory of the guided-wave poles in the complex wave number plane for this wave-guiding configuration is shown in Fig. 2(a), as the level of loss and gain is increased. When $\delta = -\delta' = 0$, we have two poles on the real axis with $\mathrm{Im}(k_x) = 0$ corresponding to the Hermitian case. Because of the nonreciprocal nature of the structure, there are no symmetric poles on the negative side of the real axis. Then, as we increase the level of loss and gain, the two poles move closer to each other until, for $\delta = -\delta' = \delta_{\mathrm{EP}} = 0.02173\omega_p$, the poles collide and merge at $k_x = 0.738\omega_p/c_0$ (red dot in the figure). Different from most previous works on non-Hermitian photonics, our exact analysis based on Green's function theory and continuum material models allows us to rigorously verify that this point of the parameter space is indeed an EP between topological modes. A necessary condition is that two first-order roots of the dispersion equation coalesce to form a second-order root, which implies that the dispersion equation at an EP should satisfy

$$D(k_{x,\mathrm{EP}}, \omega_{\mathrm{EP}}) = \frac{\partial D(k_{x,\mathrm{EP}}, \omega_{\mathrm{EP}})}{\partial k_x} = 0, \tag{2}$$

where $k_{x,\mathrm{EP}}$ and ω_{EP} are the wave number and angular frequency at which the degeneracy emerges. However, the conditions in Eq. (2) guarantee nothing more than the existence of a double root, whereas an EP should also satisfy the additional condition

$$\frac{\partial D(k_{x,\mathrm{EP}}, \omega_{\mathrm{EP}})}{\partial \omega} \frac{\partial^2 D(k_{x,\mathrm{EP}}, \omega_{\mathrm{EP}})}{\partial k_x^2} \neq 0. \tag{3}$$

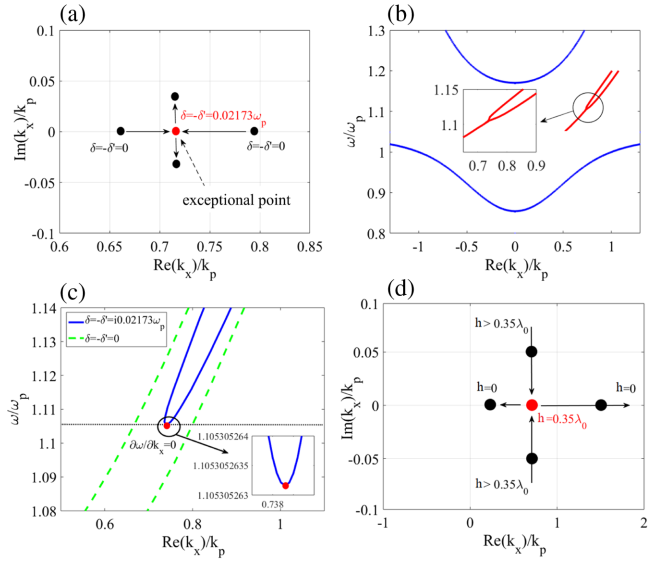

FIG. 2. (a) Evolution of the guided-wave poles in the complex wave number plane for the topological waveguide in Fig. 1, as a function of the level of loss and gain in the system (with $\omega_p/\omega_0 = 0.904$, $\omega_c/\omega_0 = 0.287$, and $h = 0.35\lambda_0$). Black dots indicate the roots of the dispersion equation. (b) Dispersion curves of the bulk modes (blue) and topological surface modes (red) for a TNT waveguide with $\omega_p/\omega_c = 3.16$, $\delta = -\delta' = \delta_{\mathrm{EP}}$, ω_p, $h = 0.63\pi c/\omega_p$, and $\epsilon_r = -1$. (c) Comparison between the dispersion curves of the topological surface modes in a Hermitian system (dashed green) and a non-Hermitian system (blue). (d) Similar to (a) but varying the isotropic spacer thickness (with $\delta = -\delta' = \delta_{\mathrm{EP}}$).

Indeed, only if Eq. (3) is satisfied, then the second-order root becomes a branch point where various branches of the dispersion function merge [38–40] (and not a saddle point of the dispersion surface). Numerical tests applied to our specific case verify that our dispersion function near the red point in Fig. 2(a) with $\omega_{\mathrm{EP}} = \omega_p/0.904$ satisfies conditions (2) and (3), fully confirming the existence of a branch point where two distinct *topological* modes coalesce. Moreover, by expanding a generic dispersion equation $D(k_x, \omega) = 0$ in a power series near k_{EP} and ω_{EP}, it is easy to show that conditions (2) and (3) are satisfied if the local structure of the dispersion equation has the form $D(k_x, \omega) = a(k_x - k_{\mathrm{EP}})^2 \pm b(\omega - \omega_{\mathrm{EP}}) = 0$, where a and b are generic complex numbers. A first-order EP is, therefore, identified as a square-root branch point of the dispersion function $k_x(\omega)$ [41–43]. Note that in our case, the dispersion function is not symmetric in k_x due to the nonreciprocal nature of the TNT waveguide. Such a nonreciprocal square-root-like structure of the dispersion function has crucial implications for the propagation properties of the proposed structure, as discussed in the following.

As we increase the level of loss and gain in the system above the critical value δ_{EP}, the EP breaks into two complex-conjugate poles [Fig. 2(a)], leading to exponentially decaying (growing) unidirectional modes propagating along the $+x$ axis. This is a typical behavior for parity-time-symmetric systems, but with the important difference that, in our case, the modes involved in this modal (phase) transition are topologically protected and backscattering immune.

Topologically protected slow-light modes.—The dispersion curves of the coupled topological surface modes are shown in Fig. 2(b), where the loss and gain level is set at the critical value δ_{EP}, clearly demonstrating the *bifurcation* of the topological surface modes (red lines) and the emergence of an EP within the band gap of the bulk modes (blue lines) [44]. For frequencies $\omega > \omega_{\mathrm{EP}}$, there are two modes with $\mathrm{Im}(k_x) = 0$, whereas for $\omega < \omega_{\mathrm{EP}}$, the modes depart from the wave number real axis and form two complex-conjugate modes with equal $\mathrm{Re}(k_x)$. In the neighborhood of the EP, the dispersion behavior is locally determined by $k_x - k_{\mathrm{EP}} \propto \sqrt{\omega - \omega_{\mathrm{EP}}}$. This relation directly implies that the dispersion curves flatten out before merging, such that $\partial_\omega k_x \to \infty$; hence, the group velocity vanishes, $v_g \to 0$. Figure 2(c) compares the dispersion of the Hermitian system with no loss or gain and the non-Hermitian system with equal amounts of loss and gain. This confirms that a waveguide working near the EP may be used to slow down and stop light, as recently observed in Ref. [45]. However, in drastic contrast with any other light-stopping system proposed so far, in our TNT waveguide, the slowing down of light is topologically protected and tunable by changing the bias. These features may suggest novel functionalities in which the propagation of an electromagnetic wave can be fully stopped and then released by varying the parameters of the system, e.g., the thickness of the waveguide, or the level of gain or loss, or the external bias, without losing any energy in unwanted backscattering, thanks to the waveguide's topological properties.

Linearly growing topological modes.—Because of its nature as a second-order singularity of the Green's function, as required by Eq. (2), an EP leads to divergence of the residue terms $w^{spp}(k_x, \omega) = N(k_x, \omega)/\partial_{k_x} D(k_x, \omega)$ in Eq. (1) associated with the two topological modes on the verge of merging. As a result, the field intensity tends to grow larger and larger as we operate closer to the EP. While no realistic structure would be able to exactly operate at the EP (any unavoidable asymmetry in the gain or loss distribution would move the EP off the real axis), it is relevant to study the evolution of the unidirectional fields as we approach the degeneracy. Figure 3 shows the magnetic field distribution in the TNT waveguide calculated exactly based on our Green's function formulation for a dipolar source at $x = 0$ at a frequency near the EP. The interference of the two excited topological waveguide modes forms unidirectional "wave packets," which become longer in length and larger in intensity as we get closer to the EP [Figs. 3(a)–3(c)]. In particular, as we approach the frequency of the degeneracy and the difference in wave

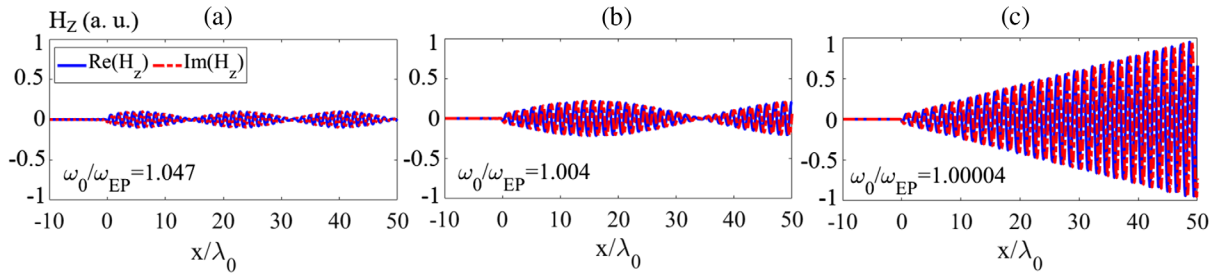

FIG. 3. Magnetic field distribution at the center of the topological waveguide considered in Fig. 2(b) excited by a dipolar source at $x = 0$ as its frequency ω_0 approaches $\omega_{EP} = \omega_p/0.904$ (exact Green's function calculations): (a) $\omega_0/\omega_{EP} = 1.047$, (b) $\omega_0/\omega_{EP} = 1.004$ and (c) $\omega_0/\omega_{EP} = 1.00004$.

number between the modes gets smaller, $\Delta k_x = k_{x,1} - k_{x,2} \to 0$, the residue terms tend to acquire a phase difference of π [13], and we can write the field distribution by Taylor-expanding Eq. (1), obtaining

$$\mathrm{Re}[H_z] \approx W(\Delta k_x)\frac{\Delta k_x x}{2}\sin\left(\frac{(k_{x,1}+k_{x,2})x}{2}\right), \qquad (4)$$

which indicates a *linearly* growing envelope modulated by a fast oscillating function, consistent with our exact calculations in Fig. 3(c). Importantly, $W(\Delta k_x)$ is a real number (related to the residue of the two poles) that becomes larger and larger as we approach the EP [13]. These results are a direct consequence of conditions (2) and (3) and indicate that, as we approach the EP from higher frequencies $\omega \to \omega_{EP}^{+}$, two oscillatory modes with constant amplitude tend to coalesce into a single linearly growing mode, also known as a Jordan mode [46–49]. Clearly, such a linear growth should not be interpreted as a form of field amplification experienced by the wave as it propagates along the structure (the wave feels no net gain, and the poles associated with the guided modes are still purely real). Our analysis indeed reveals that the linear envelope should be interpreted as the result of an interference pattern between waves with larger and larger amplitude, and closer and closer wave number, as further discussed in [13].

Topologically protected loss-immune modal transitions.—The phase transition through an EP may also be controlled by varying the thickness of the spacing layer between the two gyrotropic media. Figure 2(d) shows the guided-wave pole constellation in the complex wave number plane for different spacer thicknesses. Considering the same parameters as in Fig. 2(a) and $\delta = -\delta' = 0.02173\omega_p$, one can find an EP for $h = 0.35\lambda_0$, where λ_0 is the free-space wavelength at the source frequency, which has been set at $\omega_0 = \omega_{EP} = \omega_p/0.904$. When $h > 0.35\lambda_0$, the poles form a complex-conjugate pair; at $h = 0.35\lambda_0$, the two poles collide on the real axis (EP). Then, as $h \to 0$, the EP unfolds into two different poles moving away from each other on the real axis: one tends to $+\infty$, while the other stops at a finite positive value.

To study different waveguide configurations corresponding to the different regimes in Fig. 2(d), we performed full-wave numerical simulations using a commercial software [50]. In Fig. 4(a), we show the steady-state field distribution for a TNT waveguide with spacer thickness $h = 0$ excited by a point-dipole source. As expected, a unidirectional surface wave propagates with constant amplitude along the interface. If we then introduce a step in the wave-guiding structure, opening an opaque gap of thickness $h = 0.35\lambda_0$ between the two gyrotropic layers [Fig. 4(b)], the incident

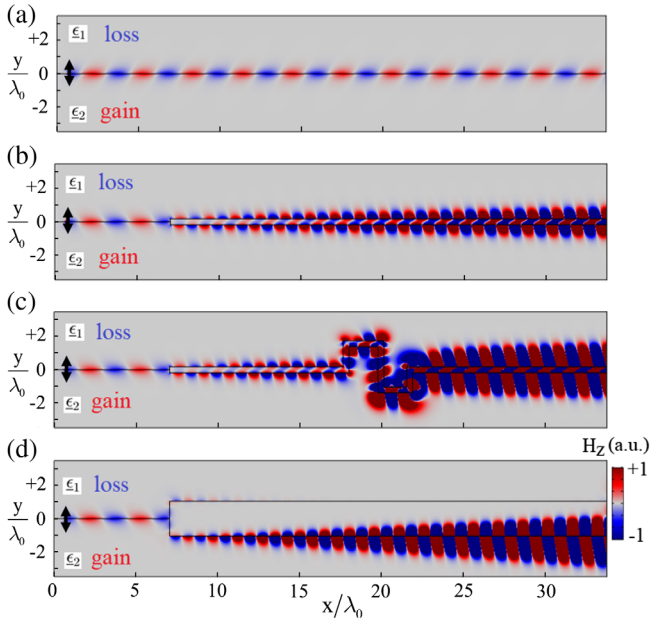

FIG. 4. Magnetic field distributions (time snapshots) in topological non-Hermitian wave-guiding structures excited by a dipolar source (black arrow). Different configurations are considered: (a) no gap between the gyrotropic layers (poles on the real axis); (b) a gap of thickness $h = 0.35\lambda_0$ is introduced (poles merge at an EP); (c) same as (b) but with a large defect along the waveguide; (d) gap of thickness $h > 0.35\lambda_0$ (complex-conjugate poles). The material parameters are the same as in Fig. 2(a) with level of loss and gain $\delta = -\delta' = \delta_{EP} = 0.021\,73\omega_p$.

wave directly "jumps" to the EP regime upon encountering the step, without any reflection because of the topological nature of the involved modes. Rather remarkably, this topologically protected modal transition directly transforms an incident surface wave into a linearly growing (Jordan) mode operating very close to an EP in the parameter space. Even more interesting, the wave continues propagating without any backscattering even in the presence of large defects [Fig. 4(c)] and grows in amplitude even in the lossy region, in drastic contrast with any conventional wave-guiding structure. For comparison, we show in Fig. 4(d) what happens if the step in the waveguide is larger, bringing the system into the regime beyond the EP, in which conventional exponentially decaying and growing waves are observed.

Conclusion.—In summary, we have theoretically demonstrated, for the first time, a non-Hermitian wave-guiding structure that exhibits an exceptional point between topologically protected modes. By operating near this degeneracy, we can realize unidirectional modes with low group velocity and inherent immunity to losses and to backscattering. This topologically protected behavior would allow rapid nonadiabatic transitions within the parameter space $\Omega = (\omega, k_x, h, \delta)$ of the wave-guiding structure, without any backscattering, as long as the initial and final states are within the bulk-mode band gap. For example, a waveguide operating far from the EP, Ω_{EP}, could be excited by a suitable temporal signal without inducing any instabilities, and then, by changing the parameters in time and/or space, the waveguide may be brought close to Ω_{EP} to take advantage of the ultralow values of group velocity in that regime. These exciting possibilities and the temporal analysis of topological non-Hermitian waveguides will be the subject of future works. In addition, while the focus of this work is on laying out a general theory of topological wave-guiding near an EP, we expect that our predictions may be experimentally tested using different realistic platforms [13].

The authors acknowledge support from the National Science Foundation (NSF) with Grant No. 1741694.

*ali.gangaraj@gmail.com
†francesco.monticone@cornell.edu

[1] D. A. B. Miller, Optical interconnects to electronic chips, Appl. Opt. **49**, F59 (2010).
[2] L. Novotny and B. Hecht, *Principles of Nano-Optics* (Cambridge University Press, Cambridge, England, 2006).
[3] C. A. Balanis, *Antenna Theory: Analysis and Design*, 3rd ed. (Wiley-Interscience, New York, 2005).
[4] A. Silva, F. Monticone, G. Castaldi, V. Galdi, A. Al, and N. Engheta, Performing mathematical operations with metamaterials, Science **343**, 160 (2014).
[5] J. D. Jackson, *Classical Electrodynamics*, 3rd ed. (John Wiley, New York, 1999).
[6] J. B. Khurgin and R. S. Tucker, *Slow Light: Science and Applications* (CRC, New York, 2008).
[7] S. Raghu and F. D. M. Haldane, Analogs of quantum-Hall-effect edge states in photonic crystals, Phys. Rev. A **78**, 033834 (2008).
[8] F. D. M. Haldane and S. Raghu, Possible Realization of Directional Optical Waveguides in Photonic Crystals with Broken Time-Reversal Symmetry, Phys. Rev. Lett. **100**, 013904 (2008).
[9] M. C. Rechtsman, Y. Plotnik, J. M. Zeuner, D. Song, Z. Chen, A. Szameit, and M. Segev, Topological Creation and Destruction of Edge States in Photonic Graphene, Phys. Rev. Lett. **111**, 103901 (2013).
[10] W. Gao, M. Lawrence, B. Yang, F. Liu, F. Fang, B. Bri, J. Li, and S. Zhang, Topological Photonic Phase in Chiral Hyperbolic Metamaterials, Phys. Rev. Lett. **114**, 037402 (2015).
[11] S. A. Skirlo, L. Lu, Y. Igarashi, Q. Yan, J. Joannopoulos, and M. Soljacic, Experimental Observation of Large Chern Numbers in Photonic Crystals, Phys. Rev. Lett. **115**, 253901 (2015).
[12] J. A. Bittencourt, *Fundamentals of Plasma Physics*, 3rd ed. (Springer-Verlag, New York, 2010).
[13] See Supplemental Material at http://link.aps.org/supplemental/10.1103/PhysRevLett.121.093901 for a thorough discussion of the Green's function extraction for the proposed topological waveguide, a general discussion of potential physical implementations, as well as a detailed analysis and interpretation of linearly growing wave propagation near the exceptional point. Supplemental Material includes Refs. [14–24]. Supplemental Material also includes time-harmonic animations for all the panels of Fig. 4.
[14] D. A. B. Miller, S. D. Smith, and A. Johnston, Optical bistability and signal amplification in a semiconductor crystal: Applications of new low-power nonlinear effects in InSb, Appl. Phys. Lett. **35**, 658 (1979).
[15] E. Palik, R. Kaplan, R. Gammon, H. Kaplan, R. Wallis, and J. Quinn, Coupled surface magnetoplasmon-optic-phonon polariton modes on InSb, Phys. Rev. B **13**, 2497 (1976).
[16] X. Zhang, Y. Li, T. Li, S. Y. Lee, C. Feng, L. Wang, and T. Mei, Gain-assisted propagation of surface plasmon polaritons via electrically pumped quantum wells, Opt. Lett. **35**, 3075 (2010).
[17] T. A. Morgado and M. G. Silveirinha, Negative Landau Damping in Bilayer Graphene, Phys. Rev. Lett. **119**, 133901 (2017).
[18] Z. Wang, Z. Wang, J. Wang, B. Zhang, J. Huangfu, J. D. Joannopoulos, M. Soljacic, and L. Ran, Gyrotropic response in the absence of a bias field, Proc. Natl. Acad. Sci. U.S.A. **109**, 13194 (2012).
[19] T. Kodera, D. L. Sounas, and C. Caloz, Magnet-less non-reciprocal metamaterials with magnetic or electric gyrotropy," in *Proceedings of 2013 URSI International Symposium on Electromagnetic Theory (EMTS) Hiroshima, Japan* (IEEE, Piscataway, NJ, 2013), pp. 397–400.
[20] N. A. Estep, D. L. Sounas, J. Soric, and A. Alu, Magnetic-free non-reciprocity and isolation based on parametrically modulated coupled-resonator loops, Nat. Phys. **10**, 923 (2014).
[21] A. B. Khanikaev, R. Fleury, S. H. Mousavi, and A. Alu, Topologically robust sound propagation in an

angular-momentum-biased graphene-like resonator lattice, Nat. Commun. **6**, 8260 (2015).
[22] R. Fleury, D. Sounas, and A. Alu, An invisible acoustic sensor based on parity-time symmetry, Nat. Commun. **6**, 5905 (2015).
[23] A. B. Khanikaev, S. Hossein Mousavi, W. K. Tse, M. Kargarian, A. H. MacDonald, and G. Shvets, Photonic topological insulators, Nat. Mater. **12**, 233 (2013).
[24] T. Ma and G. Shvets, All-Si valley-Hall photonic topological insulator, New J. Phys. **18**, 025012 (2016).
[25] S. R. Seshadri, Excitation of surface waves on a perfectly conducting screen covered with anisotropic plasma, IRE Trans. Microwave Theory Tech. **10**, 573 (1962).
[26] M. G. Silveirinha, Chern invariants for continuous media, Phys. Rev. B **92**, 125153 (2015).
[27] S. A. H. Gangaraj, A. Nemilentsau, and G. W. Hanson, The effects of three-dimensional defects on one-way surface plasmon propagation for photonic topological insulators comprised of continuum media, Sci. Rep. **6**, 30055 (2016).
[28] S. A. H. Gangaraj, M. G. Silveirinha, and G. W. Hanson, Berry phase, Berry connection, and Chern number for a continuum bianisotropic material from a classical electromagnetics perspective, IEEE J. Multiscale Multiphys. Comput. Techn. **2**, 3 (2017).
[29] S. A. H. Gangaraj and F. Monticone, Topologically-protected one-way leaky waves in nonreciprocal plasmonic structures, J. Phys. Condens. Matter **30**, 104002 (2018).
[30] The modes of the entire TNT waveguide result from the coupling of the two surface modes existing on the individual isotropic-gyrotropic interfaces. The structure respects the bulk-edge correspondence principle [7,8]: going from the lower gyrotropic medium (gap Chern number $\mathcal{C}_{\text{gap}} = -1$) to the upper gyrotropic medium ($\mathcal{C}_{\text{gap}} = +1$), through an isotropic spacer ($\mathcal{C}_{\text{gap}} = 0$), the difference in gap Chern number is $\Delta\mathcal{C}_{\text{gap}} = 2$. Hence, the bulk-edge correspondence predicts two unidirectional modes, which is indeed what we find with our exact calculations based on the system's Green's function.
[31] S. A. H. Gangaraj and F. Monticone, Coupled Topological Surface Modes in Gyrotropic Structures: Green's Function Analysis, IEEE AWPL (to be published).
[32] J. G. Van Bladel, *Electromagnetic Fields* (John Wiley & Sons, New York, 2007).
[33] M. V. Berry, Physics of nonhermitian degeneracies, Czech. J. Phys. **54**, 1039 (2004).
[34] W. D. Heiss, The physics of exceptional points, J. Phys. A **45**, 444016 (2012).
[35] P. Ambichl, K. G. Makris, L. Ge, Y. Chong, A. D. Stone, and S. Rotter, Breaking of PT Symmetry in Bounded and Unbounded Scattering Systems, Phys. Rev. X **3**, 041030 (2013).
[36] M. A. K. Othman and F. Capolino, Theory of exceptional points of degeneracy in uniform coupled waveguides and balance of gain and loss, IEEE Trans. Antennas Propag. **65**, 5289 (2017).
[37] R. El-Ganainy, K. G. Makris, M. Khajavikhan, Z. H. Musslimani, S. Rotter, and D. N. Christodoulides, Non-Hermitian physics and PT symmetry, Nat. Phys. **14**, 11 (2018).
[38] G. W. Hanson and A. B. Yakovlev, Investigation of mode interaction on planar dielectric waveguides with loss and gain, Radio Sci. **34**, 1349 (1999).
[39] G. W. Hanson and A. B. Yakovlev, An analysis of leaky-wave dispersion phenomena in the vicinity of cutoff using complex frequency plane singularities, Radio Sci. **33**, 803 (1998).
[40] A. B. Yakovlev and G. W. Hanson, Fundamental modal phenomena on isotropic and anisotropic planar slab dielectric waveguides, IEEE Trans. Antennas Propag. **51**, 888 (2003).
[41] N. Moiseyev, *Non-Hermitian Quantum Mechanics* (Cambridge University Press, Cambridge, England, 2011).
[42] A. P. Seyranian and A. A. Mailybaev, *Multiparameter Stability Theory with Mechanical Applications* (World Scientific, Singapore, 2003).
[43] A. B. Yakovlev and G. W. Hanson, Mode-transformation and mode-continuation regimes on waveguiding structures, IEEE Trans. Microwave Theory Tech. **48**, 67 (2000).
[44] A configuration with unequal loss and gain in the system never leads to an EP on the real axis because in the imbalanced case one of the poles departs from the wave number complex-plane real axis earlier than the other, and, therefore, they never coalesce to form a second-order root of the dispersion equation.
[45] T. Goldzak, A. A. Mailybaev, and N. Moiseyev, Light Stops at Exceptional Points, Phys. Rev. Lett. **120**, 013901 (2018).
[46] A linear mode of this type is also known as a Jordan mode because of the appearance of Jordan blocks in the effective Hamiltonian of the system associated with the degenerate eigenvalues that merge at the EP [47–49].
[47] S. Longhi, Spectral singularities and Bragg scattering in complex crystals, Phys. Rev. A **81**, 022102 (2010).
[48] E.-M. Graefe and H. F. Jones, PT-symmetric sinusoidal optical lattices at the symmetry-breaking threshold, Phys. Rev. A **84**, 013818 (2011).
[49] S. P. Shipman and A. T. Welters, Pathological scattering by a defect in a slow-light periodic layered medium, J. Math. Phys. (N.Y.) **57**, 022902 (2016).
[50] COMSOL MULTIPHYSICS ver. 5.3, COMSOL AB, Stockholm, http://comsol.com.